Progress In Electromagnetics Research B, Vol. 4, 41–66, 2008

ANALYTICAL STUDY OF THE INTERACTION STRUCTURE OF VANE-LOADED GYRO-TRAVELING WAVE TUBE AMPLIFIER

G. Singh

Department of Electronics and Communication Engineering
Jaypee University of Information Technology
Solan 173 215, India

Abstract—This article discusses the-state-of-the-art of the vane-loaded gyrotron traveling wave tube (gyro-TWT) amplifier, which is device of increasing importance for high resolution radar and high information density communication systems because of its high-power and broad bandwidth capabilities. Vane loading is identified as a means to achieve a low-beam energy, high-harmonic, low-magnetic field, mode-selective and stable operation of a gyro-TWT. Thus, the development of a simple approach to the analysis of the interaction structure of vane-loaded gyro-TWT has been identified as a problem of practical relevance.

1. INTRODUCTION

There are numerous applications in the millimeter and sub-millimeter wave frequency range of the electromagnetic spectrum that have led to interesting research and development activities. The existing possibilities opened up by new design tools, approaches, and electromagnetic structures will yield a continuing stream of revolutionary advances in RF vacuum tube technology. Operational demand on RF systems to achieve greater functionality, scientific innovation driven by technical opportunity, and market demand have been and continue to be the major forces behind the growth in vacuum electronic devices. These devices are used in wide variety of military and commercial applications requiring high RF power at high frequency, as well as in scientific research areas such as high-energy particle acceleration system and plasma heating for controlled thermonuclear fusion. Commercial satellite communication systems, broadcasting, industrial heating, and air traffic control radar also rely

heavily on vacuum devices for reliable performance at high power and high efficiency. In the area of sources for high resolution radar and high information density communication systems, work is now progress to improve the average power of the gyro-TWT amplifiers at millimeter and sub-millimeter wave frequencies in order to build tubes suitable for use in future radar systems, and there will probably be an attempt to improve the bandwidth beyond few GHz. The gyro-TWT is a fast wave device of the gyro-device family and based on the electron cyclotron resonance maser instability [1–68]. The benefit of the gyro-devices is derived from the combination of cyclotron resonance interaction and the fast wave interaction circuits. In the fast wave interaction circuits the electric field strength can be quite high, independent of the proximity of the metallic circuit structure. This enables the electron beam to be situated in regions of high-electric field (to produce optimum coupling) without placing the beam in close proximity to delicate circuit structures. The wavelength in gyro-devices is determined by the electron cyclotron resonance condition or more specifically, by the applied magnetic field strength [1–5]. One makes use of higher order waveguide mode in the interaction circuit, whose dimensions can be significantly larger than the operating wavelength.

The gyro-TWT is mainly consisting of MIG (magnetron injection gun), interaction structure and collector as shown in Fig. 1. A hollow beam of electrons comprised of helical beamlets of small orbital radii compared to the transverse dimensions of the interaction structure of the device, is formed normally by an electron gun, called the magnetron injection gun (MIG) — so named because of the appearance of its cathode assembly resembling a magnetron [1, 2]. Electrons are emitted from an axially symmetric emitter strip on the lateral face of a convex cathode, which is operated in the temperature-limited region rather than in the space-charge-limited region to minimize the velocity spread in the beam. Electrons are drawn off the cathode at an angle with the tube axis into a system of crossed DC electric and magnetic fields with a small angular velocity. The DC electric field is established by a potential difference between the cathode and a modulating anode, called the first anode, which may or may not be at the same or different potential from the interaction region. The required DC magnetic field for this purpose may be provided by a solenoid in the gun region as shown in Fig. 1. The gun consists of another anode called the second anode that supplies a large amount of axial energy to the beam. The trajectories of electrons become helical subject to the DC axial external magnetic field and the component of the applied electric field parallel to the magnetic line of force. In the region between the cathode

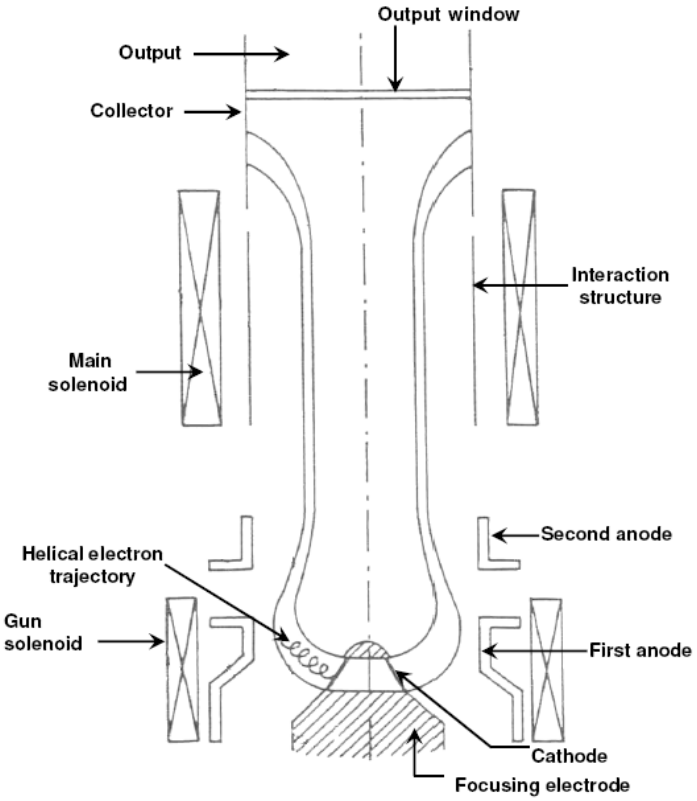

Figure 1. Schematic of the gyrotron-travelling wave tube (gyro-TWT) amplifier.

and the entrance to the interaction region, typically electrons make many gyrations. In this region the electrons are subject to a slowly increasing magnetic field. This ensures that the transformation of the axial energy of electrons into their kinetic energy is adiabatic, meaning thereby that all changes in electron motion during one gyro-cycle are relatively small. Electrons in helical trajectories formed by the gun take part in the cyclotron-resonance interaction with the transverse RF electric field of the interaction region, which is waveguide in a gyro-TWT. The spent electron beam enters a magnetic decompression region and diverges off the axis to settle on the surface of the collector surrounding the beam. The RF output is coupled out from a region further down the axis of the tube beyond an output window, which is vacuum-sealed to the tube. The output coupling arrangement has also

to provide for the necessary waveguide-mode conversion since the mode of the waveguide interaction structure could, in general, be different form that of the output wave-guiding system [1–46].

The gyro-TWT uses a non-resonant waveguide interaction structure, operates near the grazing intersection between the beam-mode line and waveguide-mode dispersion plots for wide device bandwidths [1–17]. In the device, the bunch of electrons formed by relativistic effects twists around the helix system with a pitch substantially greater than the electron pitch. The spatial position where electrons in the bunch are decelerated advances with a phase velocity approximately equal to the phase velocity of the RF wave in the waveguide, and a continuous transfer of energy takes place from the beam to the RF wave over a large interaction length. The device is operated close to the cutoff frequency of the waveguide of the constant radius portion. Due to closeness to the cutoff, the wavenumbers of the components of waves of the excited mode are small, which mitigate the effects of velocity spread in the electron beam on the inhomogeneous broadening of the cyclotron resonance band. The grazing intersection or coalescence between the beam-mode line and waveguide-mode dispersion plot yields the maximum device bandwidth as shown in Fig. 2. For wider bandwidths, however, one has to take due care to optimize the beam and magnetic filed parameters for a wide-band coalescence between the beam-mode line and waveguide-mode dispersion plots [1–41].

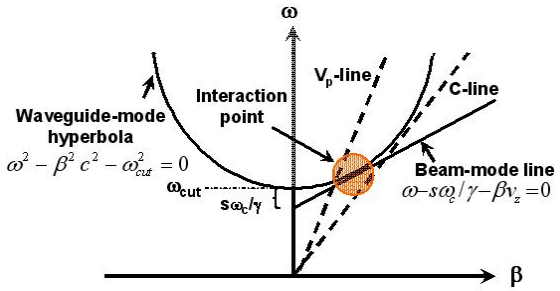

Figure 2. The waveguide and beam-mode dispersion characteristics in a gyro-TWT.

2. PROBLEM FORMULATION

Earlier, attempts were made to broadband the gyro-TWT by widening the coalescence bandwidth. For this purpose, the loading of the waveguide was suggested, for instance, by dielectric

loading [12–15], disc loading [16, 17] and helix loading [18–20]. The conventional gyro-TWTs are operated at grazing intersection for wide-band coalescence between the beam-mode and the waveguide-mode dispersion characteristics, with the beam and magnetic field parameters optimized, for wide device bandwidths as shown in Fig. 2. Although the coalescence bandwidth of the device in a smooth-wall waveguide is wider at grazing intersection than at crossing intersection, it is restricted by the rapid increase in the group velocity with frequency near cutoff where the device is operated [1–5]. The distributed gyro-TWT has a wider bandwidth than the conventional gyro-TWT though at the cost of gain [26]. Poor gain of a distributed gyro-TWT is due to a relatively small interaction length of the waveguide becoming effective for a given operating frequency, the effective length portion moving towards the smaller cross section portion of the waveguide with the increase in the operating frequency. The loaded gyro-TWT can yield wide bandwidths with a gain larger than that of a distributed gyro-TWT. A wide device bandwidth results from a wide-band coalescence brought about by dispersion shaping the waveguide by controlling the loading parameters. Thus, for instance, if a dielectric lining is used on the wall of a cylindrical waveguide, its thickness and, if a dielectric rod is used at the axis of the same waveguide, its diameter can be adjusted for this purpose [12, 14]. The method of dielectric loading however poses the problem of dielectric charging, which generates heat in the dielectric, if it is lossy. The suggested method of ameliorating the problem of dielectric charging is to coat the dielectric surface by a very thin conducting coating of thickness less than the skin depth for draining out the charge build-up [12]. Similarly, for wide device bandwidths, axially periodic discs may be arranged to load the cylindrical waveguide. For the disc-loaded gyro-TWT, the controlling parameters for widening the coalescence bandwidth and hence the device bandwidth are the disc radial thickness and the axial periodicity of discs [16, 17]. A coaxial helix internally loading a cylindrical waveguide [18–20] and a helical groove on the interior wall of a cylindrical waveguide [21, 22] can also similarly widen the coalescence bandwidth and hence broadband a gyro-TWT. For optimum performance, the device should be designed such that the desired mode dominates and suppresses all other modes during the transition of the device parameters to the operating point. Such selective excitation of the desired mode is an extremely difficult problem due to the presence of many competing modes [15, 17]. The mode, for which the self-excitation conditions will be fulfilled first during the voltage and current rise, is likely to dominate the mode competition. Other modes can be triggered, by the presence of the first

mode to reach large amplitude. So, it is important to study these effects too in order to make sure that the required mode alone dominates the mode competition. A poor coupling of the volume modes near the wall as well as a larger frequency separation between competing modes reduces the competition in a high beam harmonic operation of the device in the whispering gallery mode, the high-harmonic operation reducing the background magnetic field requirement [47, 49, 50].

The loading of a cylindrical waveguide with metal vanes projecting radially inward from the wall of the guide cannot, however, widen the bandwidth of a gyro-TWT, unlike such vane loading of the metal envelope of a conventional TWT using the helix as a sow-wave structure. This is because the azimuthally periodic vanes merely alters the cutoff frequency of a waveguide, and unlike the axially periodic discs cannot shape the dispersion characteristics and hence the coalescence bandwidth of a gyro-TWT. However, also for gyro-TWTs, the vane loading of a cylindrical waveguide was suggested but with a different purpose — to meet the challenge of building up gyrotrons with low energy beam and low magnetic field with good mode selectivity and harmonic coupling [27–29]. Moreover, if vanes are provided with the wall of the waveguide of a gyro-TWT in the large-orbit configuration, the radius of the beam of electrons circling the axis of the waveguide and interacting with the fringe field of the vanes could be reduced, that would in turn allow a reduction in beam energy. The vane-loaded structure also provides better mode selectivity in high harmonic operation. For high power gyro-TWT, the size of the waveguide is increased. An increase in the size of the waveguide reduces wall losses, but makes the interaction structure over-moded. The challenge to build gyro-TWTs with low energy beam and low magnetic field, in a high beam harmonic operation, makes a vane-loaded cylindrical waveguide an important interaction structure. The vanes, arranged at a regular angular interval around the wall of the cylindrical waveguide, create a periodic fringe field near the axis-circling electrons thus enriching the harmonic contents experienced by gyrating electrons. Thus, the harmonic coupling in a vane-loaded cylindrical waveguide is enhanced over that in a smooth-wall cylindrical waveguide. In such a gyro-TWT, the structure would reduce the required energy of beam electrons orbiting in small radii around the waveguide axis (in large-orbit configuration). Operating at a high beam harmonic requiring a reduced magnetic field, the vane-loaded gyro-TWT will also provide better mode selectivity and increased stability of the device as an amplifier.

3. INTERACTION STRUCTURE

A cylindrical waveguide, provided with wedge-shaped metal vanes projecting radially inward from the wall of the guide, excited in the transverse electric (TE) mode as shown in Fig. 3(a), was analysed. The analysis was carried out considering the angular harmonics generated due to the angular positioning of the vanes. A set of equations was generated in the Fourier amplitudes of field constants. The condition for the nontrivial solutions for the field constants gave the dispersion relation of the structure. The cold (beam-absent) analysis of a cylindrical waveguide loaded by identical wedge-shaped metal vanes, arranged around the wall of the guide, at a regular angular interval is developed. We first derive the cold dispersion relation of the vane-loaded cylindrical waveguide, excited in transverse electric (TE) mode, considering the effects of the azimuthal harmonics arising from the azimuthal periodicity of the structure [58, 70]. The azimuthal harmonics arising from the angular periodicity of vanes are taken into consideration in the field expressions. The dispersion relation of the vane-loaded cylindrical waveguide is developed with the help of the field expressions and the relevant boundary conditions.

The small-orbit configuration of the device has been considered as shown in Fig. 3(b), which is rather general, since the analytical results

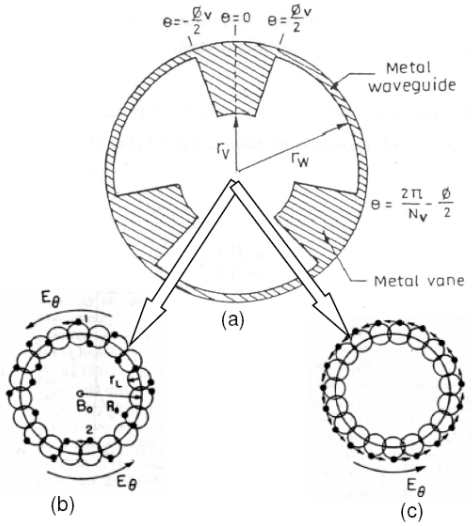

Figure 3. Transverse cross-section of (a) vane-loaded cylindrical waveguide interaction structure for (b) small-orbit configuration and (c) for large-orbit configuration.

of the large-orbit configuration as shown in Fig. 3(c) easily follow, as a special case, from those of the small-orbit configuration, by taking the hollow-beam radius tending to zero and interpreting that the Larmor radius refers to the beam position.

3.1. Cold Dispersion Relation

The method of cold (beam-absent) analysis of the vane-loaded cylindrical waveguide to take into account the azimuthal harmonic effects of the vanes closely follows that used in the past for the azimuthal harmonic effects due to the azimuthally periodic dielectric helix-supports in a conventional helix TWT [70]. The basic approach to finding the cold dispersion relation of the structure as shown in Fig. 3 (without electron beam) consists in finding a system of simultaneous equations in the Fourier components of field constants [58, 62, 70–76]. For this purpose, we follow the usual approach of substituting the field expressions in the relevant boundary conditions of the structure, and find the condition for non-trivial solution. The field expressions for the structure (Fig. 3(a)) are [58]:

$$H_{r,p} = \sum_{\nu=-\infty}^{\infty} -(j\beta/k_c)\left(A_{\nu,p}J'_\nu\{k_c r\} + B_{\nu,p}Y'_\nu\{k_c r\}\right) \quad (1)$$

$$E_{\theta,p} = \sum_{\nu=-\infty}^{\infty} (j\omega\mu_0/k_c)\left(A_{\nu,p}J'_\nu\{k_c r\} + B_{\nu,p}Y'_\nu\{k_c r\}\right) \quad (2)$$

$$H_{\theta,p} = \sum_{\nu=-\infty}^{\infty} -\left(\nu\beta/k_c^2 r\right)\left(A_{\nu,p}J_\nu\{k_c r\} + B_{\nu,p}Y_\nu\{k_c r\}\right) \quad (3)$$

where $A_{\nu,p}$ and $B_{\nu,p}$ are the field constants. $p = 1$ refers to the region 1 ($0 \le r \le r_V$; $0 \le \theta \le 2\pi$) and $p = 2$ to the region 2 ($r_V \le r \le r_W$; $\phi_V/2 \le \theta \le 2\pi/N_V - \phi_V/2$). The RF dependence $\exp j\left(\omega t - \beta z + \nu\theta\right)$ is understood. $\nu = m + kN_V$, m and k being integers. N_V is the number of metal vanes each of angular thickness ϕ_V and of inner radius r_V; and r_W is the radius of the waveguide wall (Fig. 3). J_ν and Y_ν are the Bessel functions of order ν, and of the first and second kinds, respectively. The primes with Bessel functions representthe derivative with respect to their arguments. k_c is the cutoff wavenumber. Out of the four field constants $A_{\nu,1}$, $B_{\nu,1}$, $A_{\nu,2}$ and $B_{\nu,2}$, the constant $B_{\nu,1}$ vanishes in order to prevent the field quantities from blowing up to infinity. One may choose to express the non-zero constants $A_{\nu,2}$ and $B_{\nu,2}$ in terms of $A_{\nu,1}$ with the help of

following boundary conditions:

$$E_{\theta,1} = E_{\theta,2}\,|_{r=r_V} \quad (\phi_V/2 \le \theta \le 2\pi/N_V - \phi_V/2) \tag{4}$$
$$E_{\theta,2} = 0\,|_{r=r_W} \quad (\phi_V/2 \le \theta \le 2\pi/N_V - \phi_V/2) \tag{5}$$

Two other relevant boundary conditions, which have to be used in the derivation of the dispersion relation of the structure, are:

$$H_{\theta,1} = H_{\theta,2}\,|_{r=r_V} \quad (\phi_V/2 \le \theta \le 2\pi/N_V - \phi_V/2) \tag{6}$$
$$H_{r,1} = 0\,|_{r=r_V} \quad (-\phi_V/2 \le \theta \le \phi_V/2)\,. \tag{7}$$

In order to obtain the dispersion relation, we substitute (3) into the boundary condition (6), multiply it by $\exp -j\,(\nu'\theta)$, where $\nu' = m + k'\,N_V$, and integrate it between the limits $\theta = \phi_V/2$ and $2\pi/N_V - \phi_V/2$. We then add the result thus obtained to that similarly obtained by first multiplying the boundary condition (7) — into which (1) is substituted — again by $\exp -j\,(\nu'\theta)$, and then integrating it between the limits $\theta = -\phi_V/2$ and $\theta = \phi_V/2$. The resulting equation may be divided into two parts, one corresponding to $\nu = \nu'$ and other to $\nu \neq \nu'$, and expressed as follows.

$$P_{\nu'} A_{\nu',1} + \sum_{\substack{\nu=-\infty \\ (\nu \neq \nu')}}^{\infty} Q_{\nu,\nu'} A_{\nu,1} = 0 \tag{8}$$

where

$$\left.\begin{aligned} P_{\nu'} =& \phi_V J'_{\nu'}\{k_c r_V\} + (2\pi/N_V - \phi_V)\left[(1+\eta_{\nu'})\,J_{\nu'}\{k_c r_V\}\right. \\ & \left. -\eta_{\nu'}\left(J'_{\nu'}\{k_c r_W\}/Y'_{\nu'}\{k_c r_W\}\right) Y_{\nu'}\{k_c r_V\}\right] \\ Q_{\nu,\nu'} =& \frac{\sin\left((\nu-\nu')\,\phi_V N_V/2\right)}{(\nu-\nu')\,N_V/2}\left[J'_{\nu}\{k_c r_V\} - (1+\eta_{\nu})\,J_{\nu}\{k_c r_V\}\right. \\ & \left. +\eta_{\nu}\left(J'_{\nu}\{k_c r_W\}/Y'_{\nu}\{k_c r_W\}\right) Y_{\nu}\{k_c r_V\}\right] \end{aligned}\right\} \tag{9}$$

where η_ν and $\eta_{\nu'}$ occurring respectively in the second and first equations of (9) are given by

$$\eta_{\nu,\nu'} = \frac{J'_{\nu,\nu'}\{k_c r_V\}\,Y'_{\nu,\nu'}\{k_c r_W\}}{J'_{\nu,\nu'}\{k_c r_W\}\,Y'_{\nu,\nu'}\{k_c r_V\} - J'_{\nu,\nu'}\{k_c r_V\}\,Y'_{\nu,\nu'}\{k_c r_W\}}.$$

Considering only the three close by consecutive modes of practical relevance: ν, $\nu' = \chi - 1, \chi, \chi + 1 (\nu \neq \nu')$, we may write from (9) a set of three simultaneous equations in Fourier components $A_{\chi,1}$, $A_{\chi+1,1}$

and $A_{\chi-1,1}$. The condition for the existence of the nontrivial solutions of this set of equations gives:

$$\begin{aligned} &P_\chi P_{\chi+1} P_{\chi-1} - P_\chi Q_{\chi-1,\chi+1} Q_{\chi+1,\chi-1} + Q_{\chi+1,\chi} Q_{\chi,\chi-1} Q_{\chi-1,\chi+1} \\ &-Q_{\chi+1,\chi} Q_{\chi,\chi+1} P_{\chi-1} + Q_{\chi-1,\chi} Q_{\chi,\chi+1} Q_{\chi+1,\chi-1} \\ &-Q_{\chi-1,\chi} Q_{\chi,\chi-1} P_{\chi+1} = 0 \end{aligned} \tag{10}$$

It may be shown that for practical structure dimensions the first term dominates over the remaining terms of the left-hand side of (10), so that one can write

$$P_\chi P_{\chi+1} P_{\chi-1} = 0. \tag{11}$$

Replacing χ by ν $(= m + kN_V)$, we may choose to write (11) as:

$$P_\nu P_{\nu+1} P_{\nu-1} = 0. \tag{12}$$

It has been found by actual calculation that, out of the three solutions of (12), the one that gives the solution for the desired mode is: $P_\nu = 0$. The latter may be read with the help of (9) as the following dispersion relation of the vane-loaded cylindrical waveguide:

$$\begin{aligned} &\phi_V J'_\nu \{k_c r_V\} + (2\pi/N_V - \phi_V) \left[(1+\eta_\nu) J_\nu \{k_c r_V\} \right. \\ &\left. -\eta_\nu \left(J'_\nu \{k_c r_W\} / Y'_\nu \{k_c r_W\} \right) Y_\nu \{k_c r_V\} \right] = 0 \end{aligned} \tag{13}$$

As a special case, the dispersion relation (13) for the vane-loaded cylindrical waveguide passes on to that of a smooth-wall cylindrical waveguide excited in $\mathrm{TE}_{\nu n}$ mode: $J'_\nu \{k_c r_W\} = 0$, if one puts $\phi_V = 0$ (or $r_V = r_W$). Once the value of k_c is obtained from the solution of (13), one can find the axial phase propagation constant of the structure β from the general waveguide-mode relation: $k_0^2 - \beta^2 - k_c^2 = 0$, where $k_0 (= \omega/c)$ is the free-space propagation constant, ω being the wave angular frequency, and c the speed of light.

3.2. Hot Dispersion Relation

In order to obtain the hot (beam present) dispersion relation it is further considered that RF waves interact with a thin hollow mono-energetic, relativistic, tenuous electron beam of large transverse velocities. Also it is assumed that the device operates very close to the beam-mode harmonic resonance where the cyclotron resonance maser instability prevails over the Weibel instability [1]. The current density component to be put in the wave equation is obtained from the perturbed part of the electron distribution function, the latter obtained in terms of an assumed unperturbed part of electron distribution

function by solving the relativistic Vlasov equation. A thin hollow electron beam is considered and it is assumed that the electron beam is sufficiently tenuous such that the spatial structure of the waveguide mode is unaffected due to the presence of the electron beam [4, 17, 65]. Thus, in the beam-wave coupled system of the gyro-TWT, the radial and azimuthal RF dependence of the field quantities continues to be the same as that for a cold cylindrical waveguide in the absence of the beam.

In the present analysis, let us consider a model of a thin hollow (annular) beam of monoenergetic electrons in helical trajectories all of the same Larmor radius $r_L (= p_t/m_{eo}\omega_c = p_t/|e|B_0)$ with their guiding centers uniformly distributed on a common guiding circle of radius r_H, equal to the average hollow beam radius, the radial thickness of the beam being $2r_L$. The model, though it refers to the small-orbit configuration, may be also extended to the large-orbit configuration by taking $r_H \to 0$, and a suitable value of r_L that now refers to the center of the beam position. The hot dispersion relation of the smooth wall cylindrical waveguide is as [64]:

$$\left(k_0^2 - k_z^2 - k_c^2\right) = \frac{-\mu_0 N_0 |e|^2}{\gamma m_{e0} \pi r_W^2 K_{\nu n}} \left(\frac{\eta_t^2 \left(\omega^2 - k_z^2 c^2\right) H_{\nu,-s}\left\{k_c r_H, k_c r_L\right\}}{\left(\omega - k_z v_z - s\omega_c/\gamma\right)^2} - \frac{\left(\omega - k_z v_z\right) Q_{\nu,-s}\left\{k_c r_H, k_c r_L\right\}}{\omega - k_z v_z - s\omega_c/\gamma} \right) \tag{14}$$

The dispersion relation (14) obtained as above further simplifies retaining only the first term in its right hand side that dominates over the second term, because, for a relativistic beam of large transverse velocity, the value of η_t becomes significant, and also because while the second term is inversely proportional a small quantity that tends to zero ($(\omega - k_z\, v_z - s\omega_c/\gamma) \to 0$), the first term is proportional to the square of the same small quantity.

$$\left(k_0^2 - k_z^2 - k_c^2\right) = \frac{-\mu_0 N_0 |e|^2}{\gamma m_{e0} \pi r_W^2 K_{\nu n}} \frac{\eta_t^2 \left(\omega^2 - k_z^2 c^2\right) H_{\nu,-s}}{\left(\omega - k_z\, v_z - s\omega_c/\gamma\right)^2}. \tag{15}$$

The terms in the dispersion relation (15) obtained in previous step may be suitably re-arranged.

$$\left(k_0^2 - k_z^2 - k_c^2\right)\left(\omega - k_z v_z - s\omega_c/\gamma\right)^2 = \frac{-\mu_0 N_0 |e|^2 \eta_t^2 \left(\omega^2 - k_z^2 c^2\right) H_{\nu,-s}}{\gamma m_{e0} \pi r_W^2 G_{\nu n}} \tag{16}$$

which, on substituting the expression for $G_{\nu n}$ and $H_{\nu,-s}$, given below. For weak coupling, one may set the right hand side of (16) to zero,

so that putting each of the two terms of its left hand side equal to zero, and interpreting therein $k_z \approx \beta$, one recovers the beam-mode dispersion relation and the waveguide-mode dispersion relation from the dispersion relation (16) of the gyro-TWT. It may be noted that the dispersion relation (14) was derived starting from the beam-present wave equation for a smooth-wall waveguide. However, when one takes the device in a vane-loaded waveguide, one must again start from the beam-present wave equation but now written including the azimuthal field harmonics in the field expressions. Also one has to include the presence of the azimuthal field harmonics in the solution of the Vlasov equation for the perturbation part of the electron distribution function from which to find the current density to be used in the wave equation [65]. The electron beam is represented by a distribution function in the six-dimensional spatial and momentum space. Evolution of the distribution function in the presence of RF fields is governed by Vlasov equation, which is essentially the collisionless Boltzmann equation valid under the assumed tenuous-beam approximation. One can solve Vlasov equation for the perturbed part of the electron distribution function, the product of which and the RF beam velocity component when integrated over the momentum space gives the RF beam current density component of interest involved in the beam-present wave equation. The improved approach leads to the same expression as (16) for the interaction impedance, however with the following interpretation for $G_{\nu n}$ and $H_{\nu,-s}$ [63]:

$$\left.\begin{aligned} G_{\nu n} &= \left(2/r_W^2\right)\left(\int_{r=0}^{r_V} rJ_\nu^2\{k_c r\}dr - \eta_\nu \int_{r=r_V}^{r_W} rJ_\nu^2\{k_c r\}dr \right.\\ &\qquad \left. +\eta_\nu\left(\frac{J'_\nu\{k_c r_W\}}{Y'_\nu\{k_c r_W\}}\right)\int_{r=r_V}^{r_W} rJ_\nu\{k_c r\}Y_\nu\{k_c r\}dr\right)\\ H_{\nu,-s} &= \left(UJ_{s-(\nu-1)}\{k_c r_H\} + J_{s-\nu}\{k_c r_H\}\right.\\ &\qquad \left. +VJ_{s-(\nu+1)}\{k_c r_H\}\right)J_{s-\nu}\{k_c r_H\}\,J_s'^2\{k_t r_L\} \end{aligned}\right\} \qquad (17)$$

where

$$U = -\frac{P_{\nu-1}P_\nu - Q_{\nu,\nu-1}Q_{\nu-1,\nu}}{Q_{\nu+1,\nu}P_{\nu-1} - Q_{\nu+1,\nu-1}Q_{\nu-1,\nu}}$$

$$V = \left(\frac{Q_{\nu+1,\nu-1}}{P_{\nu-1}}\right)\left(\frac{P_{\nu-1}P_\nu - Q_{\nu,\nu-1}Q_{\nu-1,\nu}}{Q_{\nu+1,\nu}P_{\nu-1} - Q_{\nu+1,\nu-1}Q_{\nu-1,\nu}}\right) - \left(\frac{Q_{\nu,\nu-1}}{P_{\nu-1}}\right).$$

The standard definite Bessel integrals occurring in (17), obtainable for

instance from [77], are:

$$\int_a^b rJ_\nu\{k_c r\}Y_\nu\{k_c r\}dr = \left[\frac{r^2}{2}\left(\left(1-\frac{\nu^2}{k_c^2 r^2}\right)J_\nu\{k_c r\}Y_\nu\{k_c r\} + J'_\nu\{k_c r\}Y'_\nu\{k_c r\}\right)\right]_a^b$$

$$\int_a^b rJ_\nu^2\{k_c r\}dr = \left[\frac{r^2}{2}\left(\left(1-\frac{\nu^2}{k_c^2 r^2}\right)J_\nu^2\{k_c r\} + J_\nu'^2\{k_c r\}\right)\right]_a^b$$

3.3. Gain for Vane-loaded Gyro-TWT

The Pierce-type gain equation may be derived from the dispersion relation (14) by an approach [59–62, 70], which is similar to what is followed in obtaining the gain equation of a conventional TWT. For this purpose, the solution of (14) is sought around the cold propagation constant β of the waveguide, such that $-jk_z = -j\beta + \beta C\delta$, with $C\delta << 1$, where C and δ are arbitrarily chosen dimensionless quantities. This enables one to express the dispersion relation (14) in the form of a cubic equation [64]:

$$\delta(\delta + jb)^2 = j \tag{18}$$

if one chooses to put $C = (KI_0/4V_0)^{1/3}$, where I_0 and V_0 are the beam current and voltage, respectively. K, which has the dimension of impedance, is identified as the interaction impedance of the gyro-TWT given by:

$$K = \frac{(\mu_0/\varepsilon_0)^{1/2}(v_t/c)^2 k_c^2\left(1+\alpha_0^2\right)H_{\nu,-s}}{\pi r_W^2 (v_z/c)\beta^4 G_{\nu n}} \tag{19}$$

where $\alpha_0\,(= v_t/v_z)$ is the beam-velocity pitch factor. The method of obtaining the gain equation of a conventional TWT from the solution of a cubic equation similar to (15) is well known. Following the same method, one may derive, from the solution of the cubic equation (18), the gain equation of a gyro-TWT. The method, which is outlined in [59–62, 70], leads to the following gain formula for a gyro-TWT in terms of the three solutions δ_1, δ_2 and δ_3, say, of (18), and x_1, the real part of δ_1, supposedly positive (corresponding to a growing wave solution):

$$G = A + BCN \tag{20}$$

where

$$A = -20\log_{10}\left|\left(1-\frac{\delta_2}{\delta_1}\right)\left(1-\frac{\delta_3}{\delta_1}\right)\right|$$
$$B = 40\pi\left(\log_{10} e\right)x_1$$

and

$$N = \beta\ell/(2\pi)$$

is the interaction length l, expressed in terms of the number of guide wavelengths. For a gyro-TWT in a vane-loaded cylindrical waveguide, one may continue to use the gain Equation (20), however, with the proper interpretation of the interaction impedance K, the latter given by (19). If one uses the 'approximate' approach, that has been followed in the past to estimate the effect of loading a gyro-TWT by a dielectric, for instance in [13], one may continue to use the expression (19) for K, but take, for β in this expression, the corresponding value for the vane-loaded cylindrical waveguide instead of that for a smooth-wall waveguide [59–62]. The value of $\beta(=(k_0^2-k_c^2)^{1/2})$ for a vane-loaded gyro-TWT in turn can be found from the solution of the cold dispersion relation of the structure (13). Thus, in this approximate approach, the effects of azimuthal harmonics due to the azimuthal periodicity of the structure enter the analysis only through the cold dispersion relation. However, an 'improved' approach to reveal the effect of fringe-field effects of vanes would be to include the effects of azimuthal harmonics not only in the cold dispersion relation but also in the beam-present (hot) dispersion relation, which can be subsequently interpreted for the device gain. In the 'improved' approach, again one may use the same gain formula as (20), that can be read with the help of the same expression (19) for the interaction impedance K, however, now with a new interpretation for $G_{\nu n}$ and $H_{\nu,-s}$ from (17). The results of both the 'approximate' and 'improved' approaches have been presented and compared in the following section. The approach would be an improvement over the approximate approach in which the azimuthal harmonic effects of azimuthally periodic vanes are included only in the cold dispersion relation and the results of the cold analysis subsequently plugged into the expression for the interaction impedance (19) that occurs in the gain equation (20) of the device. However, the axial wavenumber β that appears in the RF axial dependence, for instance in will have to be interpreted now as different from that for a cold (beam-absent) waveguide.

4. RESULTS AND DISCUSSION

The analytical method developed here includes the azimuthal harmonic effects due to the angular periodicity of vanes, though the cold (beam-absent) as well as hot (beam-present) analysis of the interaction structure. The shape of the dispersion characteristics and the value of the cutoff frequency as well as the interaction impedance characteristics of the waveguide were found to depend on the vane parameters — their number as well as radial and angular dimensions [58]. The optimum vane parameters were obtained corresponding to the minimum variation of the slope of the ω-β dispersion plot — such parameters being useful from the standpoint of the bandwidth of a gyro-travelling-wave tube using a vane-loaded cylindrical waveguide as the interaction structure. The dispersion and impedance characteristics, which were found typically for TE_{01} mode, as defined for the structure, taking four vanes, were more sensitive to the number and angular width of the vanes than to their radial depth [58]. The value of the interaction impedance, calculated at the potential beam position, was found to be higher for a loaded waveguide than for an unloaded (smooth-wall) one, and it depended on the frequency of operation relative to the cutoff. The interaction impedance also depended on the position of the beam relative to the waveguide wall where it was estimated, and hence the optimum beam position corresponding to the maximum interaction impedance was found [58]. The theory was validated against the dispersion characteristics reported elsewhere typically for four-vane magnetron-like structure excited in the 2π-mode [58]. The dependence of the dispersion and azimuthal interaction characteristics on the vane parameters, obtainable from the cold analysis of the vane-loaded cylindrical waveguide, reflects on the gain-frequency response of a vane-loaded gyro-TWT. The mode competition behaviour with respect to cold dispersion characteristics also similarly reflects on the gain-frequency response of the device [62, 65]. Thus, the interaction impedance of the device, which is found to be sensitive to the choice of the operating frequency relative to the cutoff frequency, as well as the gain of the device, becomes maximum for an optimum value of the hollow beam radius relative to the radius of the waveguide wall. It is also found that, in general, vane loading causes an increase in the gain of the device over the gain of a device in a smooth waveguide.

The vane-loaded waveguide has been referred to as the magnetron-like π- and 2π-mode structures in the literature on vane-loaded gyrotrons [39–43]. In 2π-mode excitation, the phases of RF fields in all the slots between vanes are identical, while in π-mode excitation, the phases of adjacent slots are out of phase by π. Typically, the

TE_{41} waveguide mode, which corresponds to a magnetron-like π mode, is well separated in frequency from the waveguide-modes TE_{01} and TE_{21}, corresponding, respectively, to magnetron-like 2π and π-modes, which themselves are close together in the frequency scale and competitive [65]. However, due to poor coalescence bandwidth, the vane-loaded gyro-TWT does not enjoy wide bandwidths as a dielectric-loaded or a disc-loaded gyro-TWT. Methods have been suggested as to how to widen the bandwidth of a vane-loaded gyro-TWT, which cannot be controlled by the vane parameters. Two schemes — one in a two-section configuration and the other in a tapered-cross-section (distributed-amplifier) configuration — prove to be useful in widening the bandwidth of a vane-loaded gyro-TWT at high gain values. However, the analysis of a two-section gyro-TWT has exhibited both a high gain and a wide bandwidth of the device, with a suitable choice of vane parameters of each section, along with its length and background magnetic field. In the two-section vane-loaded gyro-TWT, while, when considered individually, one of the sections shows a single peak in the gain-frequency response, the other section shows two peaks corresponding to two points of intersection between the beam-mode and waveguide-mode dispersion plots. The respective lengths of individual sections can control their gain values. By adjusting the vane parameters and magnetic field parameters, therefore, the peak of the section showing a single gain peak may be so adjusted that it falls, on the frequency scale, between the peaks of the other section showing two gain peaks. Thus, when the gain of the individual sections are added on the frequency scale, a wide-band gain-frequency response results at a high gain value, irrespective of whether one chooses to change the vane parameters of the individual sections by changing r_V/r_W, while keeping ϕ_V constant, or by changing ϕ_V, while holding r_V/r_W constant. Severing the interaction length into sections also adds to the stability of the device as an amplifier [61].

In the distributed amplification scheme of a tapered-cross section vane-loaded gyro-TWT, one may choose to taper any one of the three parameters, namely, the waveguide wall radius r_W, the vane tip radius relative to wall radius r_V/r_W, and the vane-wedge angle ϕ_V, while holding constant the remaining two [62]. Tapering of any of these parameters basically causes a tapering of the waveguide cutoff wavenumber which can be found from the solution of the cold (beam-absent) dispersion relation of the vane-loaded cylindrical waveguide. Synchronously, one has to profile the background magnetic field, say, choosing to hold the magnetic flux density relative to its grazing point magnetic flux density B_0/B_g constant, the grazing point value B_g being proportional to the waveguide cutoff frequency ω_{cut} (and hence

to cutoff wavenumber k_c) [62, 64]. Furthermore, in order to find the gain of the individual sections into which the entire interaction length is distributed, one has to take, at the concerned length portion, the appropriate values of beam parameters, namely, the relative Larmor radius r_L/r_W and the relative hollow beam radius r_H/r_W, as well as the transverse (v_t) and axial (v_z) electron velocities, and hence the beam velocity pitch factor α_0. If the radius of waveguide r_W is tapered, taking r_V/r_W and ϕ_V constant, then, with an increase taper angle, the bandwidth of the device increases, though at the cost of gain. While tapering the waveguide radius at a given taper angle, one finds that an optimum value of r_V/r_W exists that gives the widest bandwidth. Study shows that, the other types of tapering, like the tapering of r_V/r_W and that of ϕ_V, while holding r_W constant, widens the bandwidth but not as much as when the waveguide radius r_W is tapered, keeping both r_V/r_W and ϕ_V constant. Study clearly establishes that, by tapering a vane-loaded cylindrical waveguide as the interaction structure, one can widen the bandwidth of a gyro-TWT at high gain values [62]. The bandwidth of a tapered vane-loaded gyro-TWT is certainly wider than that of a non-tapered gyro-TWT, with or without vanes. The gain of a vane-loaded gyro-TWT reduces due to the tapering of cross section for wide bandwidths, but still the gain remains reasonably high — at least, as high as that of a gyro-TWT in a smooth-wall waveguide.

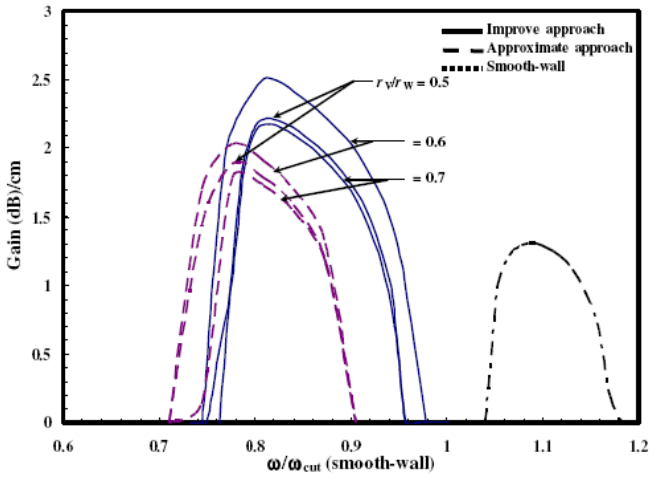

Figure 4. Gain-frequency response of vane-loaded cylindrical waveguide interaction structure for gyro-TWT and its comparisons with different approach of analysis as well as smooth wall waveguide interaction structure.

The effects of the vane parameters [67] have thus been encapsulated only in the waveguide-mode axial phase propagation constant and cutoff wavenumber, subsequently plugged into the gain equation of a gyro-TWT in an otherwise smooth cylindrical waveguide which is known as approximate approach as shown in Fig. 4. Thus the approximate method has by-passed the rigour of including the effects of azimuthal harmonics in the field expressions, both in the beam-present wave equation (from which the dispersion relation of the device is derived) and in the relativistic Vlasov equation, the solution of which gives the perturbed part of the electron distribution function, which appears in the current density components of the wave equation. The inclusion of such rigour in the analysis would have more correctly estimated the fringe-field effects of the periodic vanes which is known as improved approach as shown in Fig. 4. With the lack of this rigour, the gain value predicted by the present simplified analytical approach is bound to be approximate, though the approach has been found to be useful in searching through initial design parameters. In the large-signal regime, interactions of electrons with different waveguide-mode azimuthal harmonic components are mutually dependent, and the electron beam interacts independently with each of the azimuthal components, and thus the large-signal behaviour of a vane-loaded gyro-TWT could differ significantly from that of a smooth-wall device in which the azimuthal mode has only one component. A large-signal analysis of a vane-loaded gyro-TWT thus appears warranted.

A study of dispersion relation reveals that two types of spontaneous oscillations may be excited in a gyro-TWT amplifier, oscillation arising from the absolute instability and gyrotron backward wave oscillators. The wave amplification will occur when the beam cyclotron mode couples with the waveguide mode near the grazing intersection point. There will be a finite width of unstable spectrum about the intersection. If this unstable band is confined to the forward wave region only ($\beta > 0$), a wave will be travel down the interaction tube with convectively growing amplitude. However, if the unstable band is sufficiently wide to extend in the backward wave region ($\beta < 0$), waves growing in the backward direction will be excited and provide internal feedback to yield self-oscillation near the cutoff. If this oscillation occurs, it will grow in time (absolutely) when viewed at a fixed spatial position [48]. In addition to the self-excited oscillations caused by the absolute instability, a gyro-TWT amplifier is also susceptible to spontaneous backward wave oscillations, which occur at interaction with negative β. The critical length is very sensitive to the beam current in the low current regime. However, in the high beam current regime of interest, the critical length depends only very

weakly on the beam current. In this regime, the interaction length needs be reduced only slightly to maintain stability for a very large increase in the beam current. Using an interaction length less than the shortest critical length for all possible spontaneous oscillations, a gyro-TWT amplifier can be kept stable. If the critical length is too short to allow amplification with reasonable gain, multiple stage separated by attenuating severs can be used, where the length of each stage is still kept shorter than the critical length. This procedure will ensure single mode operation together with a high amplification gain.

5. CONCLUSION

Due to strong interaction, one may expect to achieve large gains from a vane-loaded gyro-TWT, though not as wide bandwidths (because of narrow-band coalescence between the beam-mode line and waveguide-mode dispersion plots) as those obtainable from a gyro-TWT loaded with an axially periodic disc-loaded structure. Furthermore, with a view to removing the narrow-band deficiency of the device, it will be of interest to analyse innovative device configurations, which combine the high-gain advantage of a vane-loaded gyro-TWT with any new schemes for broadbanding the device. In the scope for further work, it will be also worth making a stability analysis of the device, which has been kept outside the scope of the present work, a study which would be of relevance to a vane-loaded gyro-TWT that enjoys a higher gain than a gyro-TWT in a smooth waveguide.

REFERENCES

1. Felch, K. L., B. G. Danly, H. R. Jory, K. E. Kreischer, W. Lawson, B. Levush, and R. J. Temkin, "Characteristics and application of fast-wave gyro-devices," *Proc. IEEE*, Vol. 87, 752–781, 1999.
2. Gold, S. H. and G. S. Nusinovich, "Review of high power microwave source research," *Rev. Sci., Instrum.*, Vol. 68, 3945–3974, 1997.
3. Granatstein, V. L., B. Levush, B. G. Danly, and R. K. Parker, "A quarter century of gyrotron research and development," *IEEE Trans. Plasma Sci.*, Vol. 25, 1322–1335, 1997.
4. Rao, S. J., P. K. Jain, and B. N. Basu, "Amplification in gyro-travelling-wave tubes-dispersion relation and gain-bandwidth characteristics," *J. IETE Technical Review*, Vol. 13, 141–150, 1996.

5. Goldenberg, A. L. and A. G. Livak, "Recent progress of high-power millimeter wavelength gyrodevices," *Phys. Plasma*, Vol. 2, 2562–2572, 1995.
6. Symon, R. S., H. R. Jory, J. Hegji, and P. E. Fergusion, "An experimental gyro-TWT," *IEEE Trans. Microwave Theory Tech.*, Vol. 29, 181–184, 1991.
7. Chu, K. R., H. Y. Chen, C. L. Hung, T. H. Chang, L. R. Barnett, S. H. Chen, and T. T. Yang, "Ultra-high gain gyrotron traveling wave amplifier," *Phys. Rev. Lett.*, Vol. 81, 4760–4763, 1998.
8. Chu, K. R., H. Y. Chen, C. L. Hung, T. H. Chang, L. R. Barnett, S. H. Chen, T. T. Yang, and D. Dialetis, "Theory and experiment of ultra-high gain gyrotron traveling wave amplifier," *IEEE Trans. Plasma Sci.*, Vol. 27, 391–404, 1999.
9. Latham, P. E. and G. S. Nusinovich, "Theory of relativistic gyro-travelling wave devices," *Phys. Plasma*, Vol. 2, 3494–3510, 1995.
10. Chu, K. R., A. T. Drobot, H. H. Szu, and P. Sprangle, "Theory and simulation of gyrotron travelling-wave amplifier operating at cyclotron harmonics," *IEEE Trans. Microwave Theory Tech.*, Vol. 28, 313–317, 1980.
11. Chu, K. R., A. T. Drobot, V. L. Granatstein, and J. L. Seftor, "Characteristics and optimum operating parameters of a gyrotron travelling wave amplifier," *IEEE Trans. Microwave Theory Tech.*, Vol. 27, 178–187, 1979.
12. Leou, K. C., D. B. Mcdermott, and N. C. Luhmann, Jr., "Dielectric-loaded wideband gyro-TWT," *IEEE Trans. Plasma Sci.*, Vol. 20, 188–196, 1992.
13. Rao, S. J., P. K. Jain, and B. N. Basu, "Hybrid-mode helix-loading effects on gyro-travelling-wave tubes," *Int. J. Electron.*, Vol. 82, 663–675, 1997.
14. Rao, S. J., P. K. Jain, and B. N. Basu, "Broadbanding of gyro-TWT by dispersion shaping through dielectric loading," *IEEE Trans. Electron Devices*, Vol. 43, 2290–2299, 1996.
15. Chu, J. Y. and H. S. Uhm, "Analysis of the wide band gyrotron amplifier in a dielectric loaded waveguide," *J. Appl. Phys.*, Vol. 52, 4506–4516, 1982.
16. Leou, K. C., T. Pi, D. B. McDermott, and N. C. Luhmann, "Circuit design for a wide-band disk-loaded gyro-TWT amplifier," *IEEE Trans. Plasma Sci.*, Vol. 26, 488–495, 1998.
17. Singh, K., P. K. Jain, and B. N. Basu, "Analysis of a coaxial waveguide corrugated with wedge-shaped radial vanes considering azimuthal harmonic effects," *Progress In*

Electromagnetics Research, PIER 47, 297–312, 2004.

18. Uhm, H. S. and J. Y. Choe, "Gyrotron amplifier in a helix loaded waveguide," *Phys. Fluids*, Vol. 26, 3418–3425, 1983.
19. Choe, J. Y. and H. S. Uhm, "Theory of gyrotron amplifiers in disc or helix loaded waveguides," *Int. J. Electron.*, Vol. 53, 729–741, 1982.
20. Uhm, H. S. and J. Y. Choe, "Theory of gyrotron amplifier in a tape helix loaded waveguide," *J. Appl. Phys.*, Vol. 54, 4889–4894, 1983.
21. Cooke, S. J. and G. G. Denisov, "Linear theory of wide-band gyro-TWT amplifier using spiral waveguide," *IEEE Trans. Plasma Sci.*, Vol. 26, 519–530, 1998.
22. Denisov, G. G., V. L. Bratman, A. D. R. Phelps, and S. V. Samsonov, "Gyro-TWT with a helical operating waveguide: New possibilities to enhance efficiency and frequency bandwidth," *IEEE Trans. Plasma Sci.*, Vol. 26, 508–518, 1998.
23. Rao, S. J., P. K. Jain, and B. N. Basu, "Two-stage dielectric-loading for broadbanding a gyro-TWT," *IEEE Electron Device Letters*, Vol. 17, 303–305, 1996.
24. Nusinovich, G. S. and O. V. Sinitsyn, "Linear theory of gyro-traveling wave tubes with distributed losses," *Phys. Plasmas*, Vol. 8, 3427–3433, 2001.
25. Ganguly, A. K. and S. Ahn, "Large-signal theory of a two-stage wideband gyro-TWT," *IEEE Trans. Electron Devices*, Vol. 31, 474–480, 1984.
26. Park, G. S., J. J. Choi, S. Y. Park, C. M. Armstrong, A. K. Ganguly, R. H. Kyser, and R. K. Parker, "Gain broadening of two-stage gyrotron traveling wave tube amplifier," *Phys. Rev. Lett.*, Vol. 74, 2399–2402, 1995.
27. Chu, K. R., Y. Y. Lau, L. R. Barnett, and V. L. Granatstein, "Theory of a wide-band distributed gyrotron traveling-wave amplifier," *IEEE Trans. Electron Devices*, Vol. 28, 866–871, 1981.
28. Furuno, D. S., D. B. McDermott, C. S. Kou, N. C. Luhmann, Jr., and P. Vitello, "Theoretical and experimental investigation of a high-harmonic gyro-travelling-wave tube amplifier," *Phys. Rev. Lett.*, Vol. 62, 1314–1317, 1989.
29. Furuno, D. S., D. B. McDermott, C. S. Kou, N. C. Luhmann, Jr., and P. Vitello, "Operation of a large-orbit high-harmonic gyro-traveling wave tube amplifier," *IEEE Trans. Plasma Sci.*, Vol. 18, 313–320, 1990.
30. Chu, K. R., L. R. Barnett, W. K. Lau, L. H. Chang, and

H. Y. Chen, "A wide-band millimeter-wave gyrotron traveling-wave amplifier experiment," *IEEE Trans. Electron Devices*, Vol. 37, 1557–1560, 1990.

31. Chu, K. R., L. R. Barnett, H. Y. Chen, S. H. Chen, C. H. Wang, Y. S. Yeh, Y. C. Tsai, T. T. Yang, and T. Y. Dawn, "Stabilisation of absolute instabilities in the gyrotron travailing-wave amplifier," *Phys. Rev. Lett.*, Vol. 74, 1103–1106, 1995.
32. Chong, C. K., D. B. McDermott, and N. C. Luhmann, "Large-signal operation of a third-harmonic slotted gyro-TWT amplifier," *IEEE Trans. Plasma Sci.*, Vol. 26, 500–507, 1998.
33. Chong, C. K., D. B. McDermott, A. T. Balkcum, and N. C. Luhmann, Jr., "Nonlinear analysis of high-harmonic slotted gyro-TWT amplifier," *IEEE Trans. Plasma Sci.*, Vol. 20, 176–187, 1992.
34. Wang, Q. S., D. B. McDermott, and N. C. Luhmann, Jr., "Operation of a stable 200 kW second-harmonic gyro-TWT amplifier," *IEEE Trans. Plasma Sci.*, Vol. 24, 700–706, 1996.
35. Chong, C. K., D. B. McDermott, A. T. Lin, W. J. DeHope, Q. S. Wang, and N. C. Luhmann, Jr., "Stability of a 95 GHz slotted third-harmonic gyro-TWT amplifier," *IEEE Trans. Plasma Sci.*, Vol. 24, 735–743, 1996.
36. McDermott, D. B., B. H. Deng, K. X. Liu, J. Van Meter, Q. S. Wang, and N. C. Luhmann, Jr., "Stable 2 MW, 35 GHz, Third-harmonic TE_{41} Gyro-TWT amplifier," *IEEE Trans. Plasma Sci.*, Vol. 26, 482–487, 1998.
37. Tiong, K. K., S. P. Kuo, and S. C. Kuo, "Optimization of the design of cusptron microwave oscillators," *Int. J. Electron.*, Vol. 65, 397–408, 1988.
38. Li, H. and X. Li, "Analysis and calculation of an electron cyclotron maser having inner and outer slotted structure," *Int. J. Electron.*, Vol. 70, 213–219, 1991.
39. Chu, K. R. and D. Dialetis, "Kinetic theory of harmonic gyrotron oscillation with slotted resonant structure," *Infrared and Millimeter Waves*, Vol. 1, 45–753, Academic Press, New York, 1985.
40. Lau, Y. Y. and L. R. Barnett, "Theory of low magnetic field gyrotron (gyromagnetron)," *Int. J. Infrared and Millimeter Waves*, Vol. 3, 619–643, 1982.
41. Lau, Y. Y. and L. R. Barnett, "A low magnetic field gyrotron-gyro-magnetron," *Int. J. Electron*, Vol. 53, 693–698, 1982.
42. Destler, W. W., R. L. Weiler, and C. D. Striffler, "High-power

microwave generation from a raotating E layer in a magnetron type waveguide," *Appl. Phys. Lett.*, Vol. 38, 570–572, 1981.

43. Namkung, W., "Observation of microwave generation from a cusptron devices," *Phys. Fluids*, Vol. 27, 329–330, 1984.
44. Leou, K. C., D. B. McDermott, A. J. Balkcum, and N. C. Luhmann, Jr., "Stable high-power TE_{01} gyro-TWT amplifiers," *IEEE Trans. Plasma Sci.*, Vol. 22, 585–592, 1994.
45. Chong, C. K., D. B. McDermott, and N. C. Luhmann, Jr., "Slotted third harmonic gyro-TWT amplifier experiment," *IEEE Trans. Plasma Sci.*, Vol. 24, 727–734, 1996.
46. Menninger, W. L., B. G. Danly, and R. J. Temkin, "Multi-meagawatt relativistic harmonic gyrotron-travelling wave tube amplifier experiments," *IEEE Trans. Plasma Sci.*, Vol. 24, 687–699, 1996.
47. Kou, C. S., Q. S. Wang, and D. B. McDermott, "High power harmonics gyro-TWT's Part I: Linear theory and oscillation study," *IEEE Trans. Plasma Sci.*, Vol. 20, 155–162, 1992
48. Latham, P. E. and G. S. Nusinovich, "Stability analysis of relativistic gyro-traveling wave devices," *Phys. Plasma*, Vol. 2, 3511–3523, 1995.
49. Guo, H., S. H. Chen, V. L. Granatstein, R. Rodgers, G. Nusinovich, M. Walter, B. Levush, and W. J. Chen, "Operation of a highly overmoded, harmonic-multiplying, wideband gyrotron amplifier," *Phys. Rev. Lett.*, Vol. 79, 515–518, 1997.
50. Grow, R. W. and U. A. Shrivastava, "Impedance calculation for travelling wave gyrotrons operating at harmonics of cyclotron frequency in magnetron type circuits," *Int. J. Electron.*, Vol. 53, 699–707, 1982.
51. Park, G. S., S. Y. Park, R. H. Kyser, C. M. Armstrong, A. K. Ganguly, and R. K. Parker, "Broadband operation of Ka-band tapered gyro-travelling wave amplifier," *IEEE Trans. Plasma Sci.*, Vol. 22, 536–543, 1994.
52. Denisov, G. G., V. L. Bratman, A. W. Gross, W. He, A. D. R. Phelps, K. Ronald, S. V. Samsonov, and C. G. Whyte, "Gyrotron travelling wave amplifier with a helical interaction waveguide," *Phys. Rev. Lett.*, Vol. 81, 5680–5683, 1998.
53. McDermott, D. B., H. H. Song, Y. Hirata, A. T. Lin, T. H. Chang, H. L. Hsu, K. R. Chu, and N. C. Luhmann, Jr., "Design of a W-band TE_{01} mode gyrotron travelling wave amplifier with high-power and broadband capabilities," *IEEE Trans. Plasma Sci.*, Vol. 30, 894–902, 2002.

54. Wang, Q. S., C. S. kou, D. B. McDermott, A. T. Lin, K. R. Chu, and N. C. Luhmann, Jr., "High-power harmonic gyro-TWTs-Part II: Nonlinear theory and design," *IEEE Trans. Plasma Sci.*, Vol. 20, 163–169, 1992.
55. Lin, A. T., K. R. Chu, C. C. Lin, C. S. Kou, D. B. McDermott, and N. C. Luhmann, Jr., "Marginal stability design criteria for gyro-TWTs and comperison of fundamental with second harmonic operation," *Int. J. Electron.*, Vol. 72, 873–885, 1992.
56. Barnett, L. R., L. H. Chang, H. Y. Chen, K. R. Chu, Y. K. Lau, and C. C. Tu, "Absolute instability competition and suppression in a millimeter wave gyrotron travelling wave tube," *Phys. Rev. Lett.*, Vol. 63, 1062–1065, 1989.
57. Nusinovich, G. S. and H. Li, "Large-signal theory of gyro-travelling wave tubes at cyclotron harmonics," *IEEE Trans. Plasma Sci.*, Vol. 20, 170–175, 1992.
58. Singh, G., S. M. S. Ravi Chandra, P. V. Bhaskar, P. K. Jain, and B. N. Basu, "Analysis of an azimuthally periodic vane-loaded cylindrical waveguide for a gyro-travelling wave tube," *Int. J. Electronics*, Vol. 86, No. 12, 1463–1479, Dec. 1999.
59. Singh, G., S. M. S. Ravi Chandra, P. V. Bhaskar, P. K. Jain, and B. N. Basu, "Control of gain-frequency response of a vane-loaded gyro-TWT by beam and magnetic field parameters," *Microwave Optical and Technology Letters*, Vol. 24, No. 2, 140–145, Feb. 2000.
60. Agrawal, M., G. Singh, P. K. Jain, and B. N. Basu, "Two-stage vane loading of gyro-TWT for high gains and bandwidths," *Microwave Optical and Technology Letters*, Vol. 27, No. 3, 210–213, March 2000.
61. Agrawal, M., G. Singh, P. K. Jain, and B. N. Basu, "Analysis of tapered vane loaded broad band gyro-TWT," *IEEE Trans. Plasma Science*, Vol. 29, No. 3. 439–444, March 2001.
62. Singh, G., S. M. S. Ravi Chandra, P. V. Bhaskar, P. K. Jain, and B. N. Basu, "Analysis of vane-loaded gyro-TWT for the gain-frequency response," *IEEE Trans. Plasma Science*, Vol. 32, No. 5, 2130–2138, May 2004.
63. Singh, G. and B. N. Basu, "Improved approach for the gain-frequency response of vane-loaded gyro-TWT," *IEEE Trans. Plasma Science*, Vol. 33, No. 4, 1443–1446, August 2005.
64. Singh, G., M. V. Kartikeyan, A. K. Sinha, and B. N. Basu, "Effects of beam and magnetic field parameters on highly competing TE_{01} and TE_{21} modes of vane loaded Gyro-TWT," *Int. J. Infrared and Millimeter Waves*, Vol. 23, No. 4, 517–533, April 2002.

65. Singh, G., M. V. Kartikeyan, and B. N. Basu, "Gain-frequency response of nearby waveguide mode in vane-loaded gyro-TWTs," *IEEE Trans. Plasma Science*, Vol. 34, No. 6, 554–558, June 2006.
66. Singh, G. and M. V. Kartikeyan, "Optimization of vane parameters for the gain-frequency response of a vane-loaded gyro-TWT," *Int. J. Infrared and Millimeter Waves*, Vol. 26, No. 2, 247–261, February 2005.
67. Singh, G., M. V. Kartikeyan, and G. S. Park, "Gain and bandwidth analysis of vane-loaded gyro-TWT," *Int. J. Infrared and Millimeter Waves*, Vol. 27, No. 3, 333–341, March 2006.
68. Singh, G. and B. N. Basu "Modal analysis of azimuthally periodic vane-loaded cylindrical waveguide for gyro-TWT," *Progress In Electromagnetics Research*, PIER 70, 175–189, 2007.
69. Lee, H. S., "Dispersion relation of corrugated circular waveguides," *Journal of Electromagnetic Waves and Applications*, Vol. 19, No. 10, 1391–1406, 2005.
70. Basu, B. N., R. K. Jha, and L. Kishor, "Electromagnetic wave propagation through an azimuthally perturbed helix," *J. Appl. Phys.*, Vol. 8, 3625–3627, 1985.
71. Khalaj-Amirhosseini, M., "Analysis of longitudinally inhomogeneous waveguides using the Fourier series expansion," *Journal of Electromagnetic Waves and Applications*, Vol. 20, No. 10, 1299–1310, 2006.
72. Hernandez-Lopez, M. A. and M. Quintillan-Gonzalez, "A finite element method code to analyze waveguide dispersion," *Journal of Electromagnetic Waves and Applications*, Vol. 21, No. 3, 397–408, 2007.
73. Park, J. K. and J. N. Lee, "A full wave analysis of a coaxial waveguide slot bridge using the Fourier transform technique," *Journal of Electromagnetic Waves and Applications*, Vol. 20, No. 2, 143–158, 2006.
74. Yener, N., "Algebaric function approximation in eigen value problem of lossless metallic waveguide: Examples," *Journal of Electromagnetic Waves and Applications*, Vol. 20, No. 6, 731–745, 2006.
75. Yener, N., "Advancement of algebaric function approximation in eigen value problems of lossless metllic waveguidses to infinite dimensions, part I: Properties of the operation in infinite dimensions," *Journal of Electromagnetic Waves and Applications*, Vol. 20, No. 12, 1611–1628, 2006.

76. Yener, N., "Advancement of algebaric function approximation in eigenvalue problems of lossless metallic waveguides to infinite dimensions, part III: Examples verifying theory," *Journal of Electromagnetic Waves and Applications*, Vol. 20, No. 13, 1861–1874, 2006.
77. McLachlan, N. W., *Bessel Functions for Engineers*, Clarendes, Oxford, UK, 1943.